HYGROTHERMAL BEHAVIOR MODELING OF DIFFERENT LIME-HEMP CONCRETE MIXES
ICCS13 CONFERENCE PROCEEDINGS

Samuel DUBOIS
Ph.D Student, F.R.I.A Grant holder, Dept. of Environmental Sciences and Technologies, Gembloux Agro-Bio Tech, University of Liège, Belgium

Frédéric LEBEAU
Professor, Dept. of Environmental Sciences and technologies, Gembloux Agro-Bio Tech, University of Liège, Belgium

ABSTRACT:
This paper studies the specific hygrothermal behavior of Lime-Hemp concretes through analysis of non-linear coupled heat and moisture transfer using a research model. Three compositions were studied, varying the type of binder. First *Moisture Buffer Value* determination tests are lead experimentally using the NORDTEST protocol. These dynamic experiments, which reveal the moisture storage and exchange capacity together with latent heat effects, are then modeled using a set of partial differential equations. The reduction of humidity buffering capacity induced by hydraulic binder incorporation is properly evaluated and the hygrothermal parameters can be assessed by inverse modeling.

Keywords: Moisture Buffer Value, Lime-Hemp concrete, HAM Modeling, Inverse Modeling

1. INTRODUCTION

Lime-Hemp Concretes (LHC) gained success in the last decade in the context of sustainability achievement objectives in the building sector. These hygroscopic construction materials are generally made of a lime-based binder and hemp particles mixed in different proportions according to final usage [1] (Figure 1). They are stated to offer a good regulation capacity of the indoor humidity [2], improving comfort for occupants [3]. The way to put this particular regulation behavior into evidence is to evaluate the moisture buffer capacity, i.e. the moisture exchange capacity under a dynamic exposure to relative humidity (RH) cycle. The relative humidity variations can be caused either by temperature change of the ambient air or through adding of moisture to it.

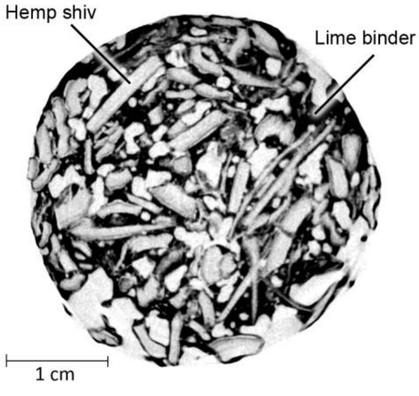

Fig.1 X-Ray Tomography slice of a Lime-Hemp bloc, a "wall-mix"

The NORDTEST project [4] has been one of the first attempt to find a consensus for an experimental protocol able to characterize adequately this buffer capacity through the definition of a global parameter called the Moisture Buffer Value (MBV). Beside the direct humidity regulation that is evaluated by the MBV, the buffer performance of hygroscopic materials also causes latent heat effects whose impact on energy balance is still not well understood.

Along with the will to characterize porous hygroscopic materials like LHC experimentally, the modeling of their behavior has progressed substantially in the last decades [5-8]. Indeed, Heat Air and Moisture (HAM) models which deal with detailed hygrothermal analysis of porous materials have gained a lot of accuracy through the development of computer power and a better knowledge of the involved phenomena. Till today, many HAM computer software's were developed for building applications and some commercialized [9-10]. Their main difference is to be found in the description of the moisture flows that can have several levels of complexity, ranging from diffusivity models using moisture content as driving potential to conductivity model using the actual thermodynamic driving potential and separated liquid and vapor flows [11]. All these models rely however on materials and boundary conditions parameters, most of them being time consuming to obtain.
The computation of temperature and moisture content fields in building materials, from the known parameters and boundary conditions forms a *direct HAM problem* [12]. There exist however several methods that allow

parameters estimation from temperature and moisture content fields measurements, which constitutes an *inverse HAM problem*. Among these inverse modeling methods, the Bayesian approaches are becoming more and more popular in environmental models. In Bayesian optimization, parameters are not unknowns with fixed values but stochastic variables whose distributions have to be specified. The distribution given before estimation is called "prior" and the distribution given after integration of the experimental data is called "posterior". Historically, the emergence of the Markov Chain Monte Carlo (MCMC) simulations with the Random Walk Metropolis algorithm as first widely used approach [13] have greatly simplified the estimation of posterior distribution of parameters. Recently, [14] developed the Differential Evolution-Markov Chain (DE-MC) method, able to run simultaneously several Markov chains, for global parameter space exploration, and using a so called "genetic" algorithm for parameter estimation evolution. The Differential Evolution Adaptive Metropolis (DREAM) algorithm [15-16] is an evolution of the DE-MC, able to automatically tunes the scale and orientation of the proposal distribution during the evolution of posterior distribution.

The goal of this paper is (1) to measure the moisture buffer value of samples with different binder compositions and more particularly assess the impact of hydraulic binder dosage on moisture exchange capacity and latent heat effects, (2) Confront a HAM model to the data acquired experimentally through an inverse modeling approach using DREAM algorithm.

2. THE MOISTURE BUFFER VALUE

The need for a standardized parameter to characterize the moisture buffering capacity of materials led to the definition of the Moisture Buffer Value (MBV) during the NORDTEST project [4] together with the proposal of a dynamic experimental protocol for materials classification. The practical MBV is defined as : *"the amount of water that is transported in or out of a material per open surface area, during a certain period of time, when it is subjected to variations in relative humidity of the surrounding air"* [4]. Concretely, the samples are subjected to cyclic step changes in relative humidity (RH) at a constant temperature of $23\,°C$ and are weighted regularly. The cycle is composed by moisture uptake during 8 hours at 75% RH followed by moisture release 16 hours at 33% RH and is repeated until constant mass variation between 2 consecutive cycles is reached. The practical MBV in $kg/(m^2 \cdot \%RH)$ is then given by Eq.1.

$$MBV_{practical} = \frac{\Delta m}{A \cdot \Delta RH} \qquad (1)$$

where Δm is the mass variation during the 8 hours absorption phase or the 16 hours desorption phase in one complete cycle, $A\,[m^2]$ is the total exchange surface and ΔRH is the difference between the high and low relative humidity of the cycle. This experimental value is a direct measurement of the amount of moisture transported to and from the material for the given exposure cycle.

A theoretical value of the MBV, called the ideal MBV, can be computed analytically using semi-infinite solid theory and Fourier series without transfer resistance at exchange surface [4] :

$$MBV_{ideal\,75-33} = 0.00568 \cdot p_{sat} \cdot b_m \cdot \sqrt{24 \cdot 3600} \qquad (2)$$

with the saturation vapour pressure equal to $3145\,Pa$ at $23\,°C$. As one can see, this value is proportional to the moisture effusivity $b_m\,[kg/(m^2 \cdot Pa \cdot s^{0.5})]$, a parameter based on standard steady-state hygric material parameters :

$$b_m = \sqrt{\frac{\delta_v \cdot \rho_l \cdot \frac{\partial \theta}{\partial \varphi}}{p_{sat}}} \qquad (3)$$

where $\delta_v\ [kg/Pa.m.s]$ is the vapor permeability of the material. The slope of the moisture storage curve, $\partial\theta/\partial\varphi$, is generally called the moisture capacity ξ, expressed here in $[m^3/m^3]$. There is always a disagreement between measured and analytically calculated MBV_{ideal} due to the dynamic nature of the experimental protocol, film resistance on specimen exchange surface and deviations from the typical step transitions.

For LHC, the MBV_{ideal} can be evaluated using hygric parameters measured by A. Evrard [1]. The result is given in table 1 for a sample made of preformulated lime (*Tradical PF70*) and hemp particles mixed in "wall-mix" proportions.

Table 1 Hygric parameters for a LHC wall-mix (Evrard, 2010)

δ_v	$\xi_{30-80\%RH}$	b_m	MBV_{ideal}
$\frac{kg}{Pa}.m.s$	m^3/m^3	$kg/(m^2.s^{0.5}.pa)$	$g/(m^2 \cdot \%RH)$
3.77E-11	0.040	6.92E-7	3.61

3. TEST PROGRAMS

3.1 Samples

The MBV determination is led on 3 different blocs with typical mass proportions of constituents corresponding to a wall-mix. The binder of the first sample is made of 35% Portland cement and 65% calcic lime, 65% Portland cement and 35% calcic lime for the second, and 100% quick setting cement for the last one. The hemp is produced in France and commercialized under the name *Chanvribat*. The mix proportions used for the 3 samples are summarized in Table 2, expressed in terms of mass of the different components to produce $1\,m^3$ of final material.

Table 2 Samples and mix proportions (for 1m³)

	Water	Calcic lime	Cement	QS Cement	Hemp shivs	Total
unit	kg	kg	kg	kg	kg	kg
LH	302.4	163.8	88.2	0	120	674.4
CH	302.4	88.2	163.8	0	120	674.4
QSH	296	0	0	216	120	632

The LHC sample blocs have all three an unique moisture exchange surface of approximately $0.0225m^2$ and a thickness of $0.150m$, which is stated sufficient given the theoretical moisture penetration depth during the MBV experiment. Lateral and back faces are isolated from water exchange with polyethylene film and tape. Before the test, the samples are maintained in a constant relative humidity chamber at 50% RH for 4 days. Table 3 gives the volume of the samples, their true exchange surface area, their dry density and the water content before the test for the 3 tested samples.

Table 3 Properties of the tested samples

	Volume of sample	Exchange surface area	Dry density	Water content before test
unit	m^3	m^2	kg/m^3	m^3/m^3
LH	3.51E-3	0.02265	383.5	31.9
CH	3.63E-3	0.0234	422.9	40.2
QSH	3.53E-3	0.02295	396.9	39.1

3.2 Test platform

A HPP749 (*Memmert*) climatic chamber was used to carry out the humidity cycles in an isothermal closed environment. As the average air velocity in the chamber is necessary to estimate the vapour diffusion resistance factor at the surface of the material, it was measured in the horizontal direction with an hot-wire anemometer 8465-300 (*TSI*). It showed an average value of $0.135 \pm 0.03\, m/s$.

Three SHT75 (*Sensirion*) sensors are implemented, 5, 10 and 15 cm above the sample in order to monitor the evolution of humidity and temperature in the chamber. Finally, a thermocouple is placed on the surface of the material with a small thermal insulation cap on top of it. This sensor is dedicated to highlight latent heat effects. The insulation cap is stated necessary to monitor the actual surface temperature, avoiding the influence of the surrounding air. Once instrumented, the sample is placed inside the chamber on a M-Power (*Sartorius*) laboratory scale with a 0-3100 g range and 0.01 g resolution. This scale is monitored every 5 minutes trough its RS232 output via a *LabVIEW* acquisition program. The experimental set-up is shown on Figure 2.

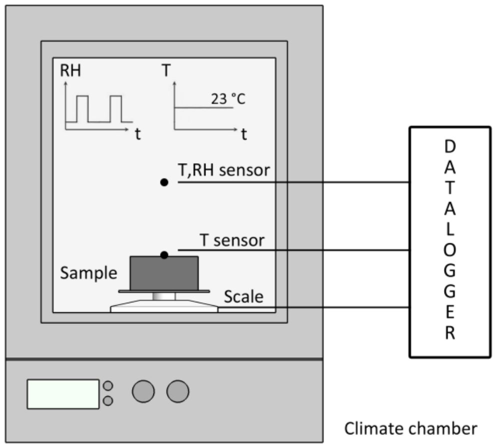

Fig.2 Experimental set-up

Figure 3 shows the measured ambient relative humidity and temperature in the chamber during a typical experiment. The indicated values for humidity and temperature are the means of the measurements of the three *Sensirion* sensors. Number are assigned to each of the 24h cycles to facilitate the subsequent analyzes. For each cycle, the climatic chamber is performing a 33-70% RH transition in 60 minutes and 75-50% RH in 150 minutes. The ends of the two transitions are really slow. The humidity cycle needs further improvement to get closer to a step solicitation. The actual humidity values are also higher than excepted, with an average of 40% during the low humidity phase (16 hrs) and 75.3% during the high humidity phase (8 hrs). This is partly due to poor calibration of the humidity sensors regulating the chamber. It is then necessary to take into account these conditions during the computer simulation and the MBV determination. Therefore the choice has been made to use the actual RH and temperature values as input for boundary conditions during the modelling phase instead of ideal step transitions for humidity and constant value for temperature.

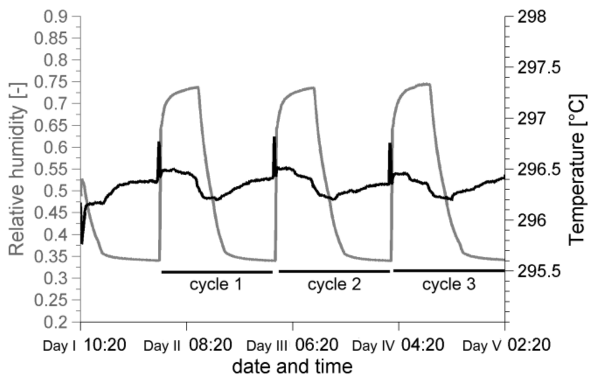

Fig.3 Ambient conditions in the chamber

4. THE HYGROTHERMAL MODEL

Modeling the hygrothermal behavior of the LHC sample during the MBV determination experiment is considered here a tool for parameter estimation through an inverse modeling approach. The HAM model is developed in *COMSOL Multiphysics* and interoperable with the inverse modeling tool that is encoded in *Matlab* and presented in the next section.

The following hypothesis are taken for the mathematical description of heat and mass transfer :
(1) The material is non-deformable and isotropic; (2) the fluid phases do not chemically react with the solid matrix; (3) The dry air pressure is constant (no air advection) and the total gas pressure gradients are considered negligible; (4) no liquid transport is considered and vapor pressure is the only driving potential for moisture movement; (5) there is a local thermodynamic equilibrium between the different phases; (6) There is no thermal effects due to friction or compression; (7) thermal diffusion (Soret effect) is neglected; (8) no hysteresis phenomena is accounted for. The two descriptive variables chosen for this problem are temperature $T\ [K]$ and relative humidity $\varphi\ [-]$ and it will be solved in 1D.

Even if the experiment is conducted in isothermal conditions, the heat balance equation is necessary to account for latent heat effects in the material. No source terms are necessary is this study case and water is consider as pure water with liquid density $\rho_l = 1000\ kg/m^3$ and latent heat of vaporization $L = 2257\ kJ/kg$.
The mass and energy conservation equations are in consequence encoded as follow :

$$\xi \cdot \rho_l \cdot \frac{\partial \varphi}{\partial t} = \delta_v \cdot \frac{\partial^2(\varphi \cdot p_{sat})}{\partial x^2} \qquad (4)$$

$$\rho c \frac{\partial T}{\partial t} = \frac{\partial}{\partial x}\left(\lambda \frac{\partial T}{\partial x} + \delta_v \cdot \frac{\partial(\varphi \cdot p_{sat})}{\partial x} \cdot L\right) \qquad (5)$$

where,

λ : Thermal conductivity $[W/(mK)]$ considered constant
ξ : The moisture capacity $[m^3/m^3]$ considered constant for the given RH interval.
c : Material heat capacity $[J/kgK]$ considered constant
p_{sat} : Vapor saturation pressure $[Pa]$, temperature-dependent

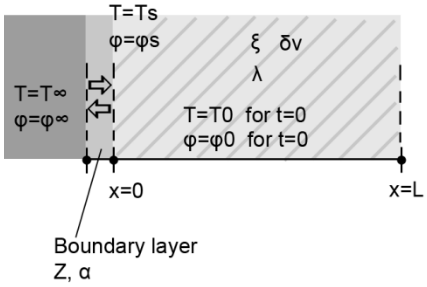

Fig.4 1D representation of sample bloc with boundary layer

Referring to Figure 4, we can write the following boundary and initial conditions for moisture transport :

$$(g_v) \cdot \vec{x} = \frac{(\varphi_\infty p_{sat,\infty} - \varphi_s p_{sat,s})}{Z_s} \qquad x = 0 \qquad (6)$$

$$\frac{\partial \varphi}{\partial x} = 0 \qquad x = L \qquad (7)$$

$$\varphi(x, 0) = \varphi_0 \qquad 0 < x < L \qquad (8)$$

where,

g_v : The moisture flux density $[kg/m^2\, s]$
$\varphi_\infty, p_{sat,\infty}$: Ambient relative humidity and saturation pressure
$\varphi_s, p_{sat,s}$: Relative humidity and saturaition pressure at the exchange surface
Z_s : Vapor diffusion resistance factor $[Pa/(kg \cdot m^2 \cdot s)]$

The vapour diffusion resistance factor characterizes the moisture transfer resistance that exists on the material surface and slows down the moisture exchange. Its value is generally fixed to 5E7 $Pa/(kg \cdot m^2 \cdot s)$ which is the usually accepted value for environments with an ambient air velocity around $0.1\ m/s$ [Rode et al., 2005]. It's similar to a value of $Z_{s,v} = 360\ s/m$ when the surface flux density is written in terms of absolute humidity :

$$(g_v) \cdot \vec{x} = \frac{(v_\infty - v_s)}{Z_{s,v}} \qquad (9)$$

To calculate the accumulated moisture, Eq. 10 is used.

$$G_v(t) = \int_0^t g_v dt \qquad (10)$$

The resulting relative weight of the sample is given by :

$$m(t) - m_0 = G_v(t) * A \qquad (11)$$

where,

$m(t)$ is the weight of the sample at time t $[kg]$
m_0 is the initial weight of the sample $[kg]$
A is the exchange surface area of the sample $[m^2]$

For heat transport, the boundary and initial conditions are given by :

$$(\vec{q})\cdot\vec{x} = \alpha\cdot(T_\infty - T_s) + \beta\cdot L\cdot(\varphi_\infty p_{sat,\infty} - \varphi_s p_{sat,s})/Z_s \qquad x = 0 \qquad (12)$$

$$(\vec{q})\cdot\vec{x} = \alpha\cdot(T_\infty - T_L) \qquad x = L \qquad (13)$$

$$T(x,0) = T_0 \qquad 0 < x < L \qquad (14)$$

where,

$\vec{q}$: heat flux density $[W/m^2]$
T_∞ : Ambient temperature
T_s : Temperature at exchange surface
T_L : Temperature at the bottom of the sample
α : Convective heat transfer coefficient $[W/m^2K]$

The convective heat transfer coefficient fixed to $1{,}44E8/Z_s$ according to [4].
The input data T_∞ and φ_∞ for ambient air variations used as boundary solicitation in the model are the measured RH and temperature from the experimental cycles, which as mentioned before are quite different from the ideal step cycle (Figure 3).

5. INVERSE MODELLING

The recently developed DREAM algorithm [16] will be used in order to get an estimation of different parameters of the HAM model, so that the simulation is as close as possible to the experimental data sets. The surface temperature, that was monitored during MBV determination, is governed mainly by latent heat effects. The thermal conductivity and capacity were proven to be impossible to estimate from this temperature data set. In consequence, we will use the values measured by Evrard [1] for these 2 thermal parameters during the simulation. Furthermore, the optimization will be led using only the relative weight variation data set. The optimized parameters are thus all linked to moisture transfer :

- Hygric parameters : the vapor permeability of the sample δ_v and its hygric capacity ξ
- Boundary and initial conditions : the vapor diffusion resistance factor at exchange surface Z_s and the initial equilibrium RH in the sample φ_0

Table 4 gives the prior distribution of these parameters, consisting of uniform distribution limited by values defined as "realistic" knowing previous studies on LHC and experimental conditions. The vapor permeability of the sample is expressed here in terms of vapor resistance factor $\mu = \frac{\delta_v}{\delta_a}\,[-]$ where δ_a is the vapor permeability of dry air.
DREAM algorithm will output the posterior distribution of parameters, i.e. the probability distribution of tested parameters values during the evolution of the optimization. On this basis, it's possible to get the final estimation for each parameter by computing the mean value of last elements of all Markov chains.

Table 4 Prior uniform distribution of parameters

	Z	μ	ξ	φ_0
unit	$Pa/(kg\cdot m^2\cdot s)$	$-$	m^3/m^3	$-$
	[1E7-1E8]	[1-10]	[0.01-0.1]	[0.5-0.65]

6. RESULTS

6.1 Experimental phase

The relative weight variation of the samples during the MBV characterization and for the 3 first complete humidity cycles are given on Figure 5. The surface temperature of the samples during the same cycles is shown on Figure 6. At first glance, it seems that the different mixes behave in a similar way in terms of moisture transfers.

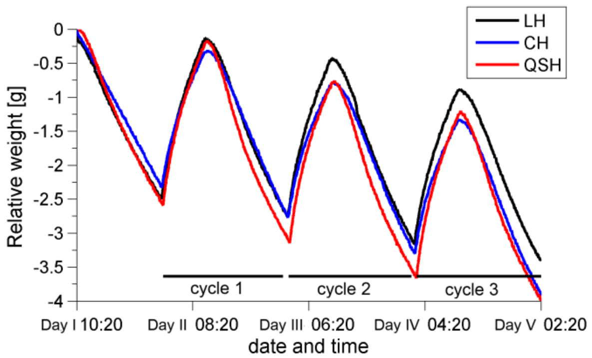

Fig.5 Relative weight evolution of the samples during 3 full RH cycles

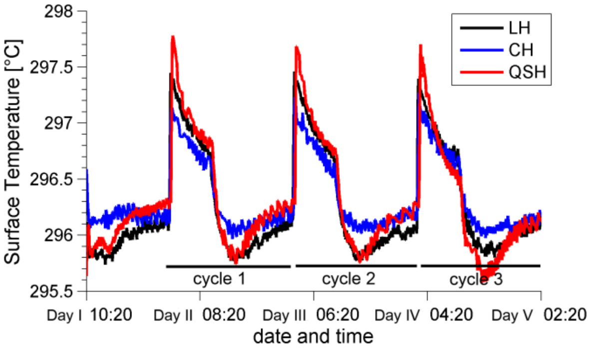

Fig.6 Surface temperature of the samples during 3 full RH cycles

Table 4 shows the comparison between the different samples in terms of $MBV_{practical}$ (Eq. 1). The results are expressed for the three cycles on Fig. 3, with a value for absorption phase, another for desorption phase and the mean on the cycle. The practical buffer value measured for the LH sample, with a global mean on 3 cycles of $3.06\,g/(m^2\,\%RH)$, is close to the ideal MBV calculated from [1]. In fact the samples used in Evrard [1] and the LH sample are very similar, since the preformulated lime *Tradical PF70* is made of 75% calcic lime, 15% ordinary Portland cement and 10% pouzzolanic additives. The surface resistance effects can explain why the ideal MBV is higher than the measured MBV. The CH sample shows a practical MBV of $2.71\, g/(m^2\,\%RH)$, a reduction of approximately 11% in comparison to LH sample. Finally, the measured mean practical MBV of the QSH sample is $3.20\, g/(m^2\,\%RH)$, 5% more the LH sample. However, referring to Table 2, this bloc has proportionally more hemp that the two others. This could explain why the MBV is lightly greater.

Table 4 $MBV_{practical}$ $[\boldsymbol{g/m^2 \cdot \%RH}]$ results for the experimental data sets

	ΔRH	Cycle 1			Cycle 2			Cycle 3		
		Abs.	Des.	Mean	Abs.	Des.	Mean	Abs.	Des.	Mean
LH	~35.3%	2.91	3.21	3.06	2.86	3.40	3.13	2.84	3.13	2.98
CH	~35.3%	2.43	2.95	2.69	2.40	3.04	2.72	2.35	3.11	2.73
QSH	~35.3%	2.96	3.60	3.28	2.83	3.47	3.15	2.94	3.42	3.18

6.2 Modeling phase

The Figure 7 presents the posterior probability distribution function of the 4 optimized parameters for 4000 evaluations of the COMSOL model with 10 Markov chains. Because of similarity between the tested samples we will focus only on the LH experiment data set.

It's immediately striking that vapor resistance factor of the sample is strongly correlated to its moisture capacity. It can be understood clearly by looking at Eq. 4, where the two constant parameters can be combined in one unique value, the moisture diffusivity. As a result, the estimated values for these 2 parameters are arbitrary and only the ratio binding them can be evaluated accurately. The correlation between the moisture capacity and the vapor resistance factor of the sample can be evaluation by linear regression. The relation obtained is :

$$\xi = 0.0093 \cdot \mu + 0.0016 \qquad (15)$$

A further step of the research would be to measure experimentally the two parameters on the 33-75%RH range in order to validate this relation.

On the other hand, the initial RH in the sample and the surface resistance factor have really compact distribution function and it seems they can be evaluated precisely.

Table 5 gives the mean estimates for all 4 parameters, i.e. the mean of the 20 last estimated parameter values of the 10 Markov chains.

Table 5 Mean best estimate of optimized parameters

	Z	μ	ξ	φ_0
unit	$Pa/(kg \cdot m^2 \cdot s)$	–	m^3/m^3	–
LH	4.43E7	3.37	0.033	0.5964

The comparison between measurement data and the model with the mean best estimates of parameters is shown on Figure 8. The HAM seems able to describe adequately the moisture behavior of the LH bloc during a MBV experiment. Figure 9 shows the surface temperature predicted by the model with the optimized parameters for hygric transfers and approximated constant values for heat tranfer parameters ($\lambda = 0.1 W/(mK)$, $c = 1560 J/(kgK)$ and $\alpha = 1{,}44E8/Z_s$).

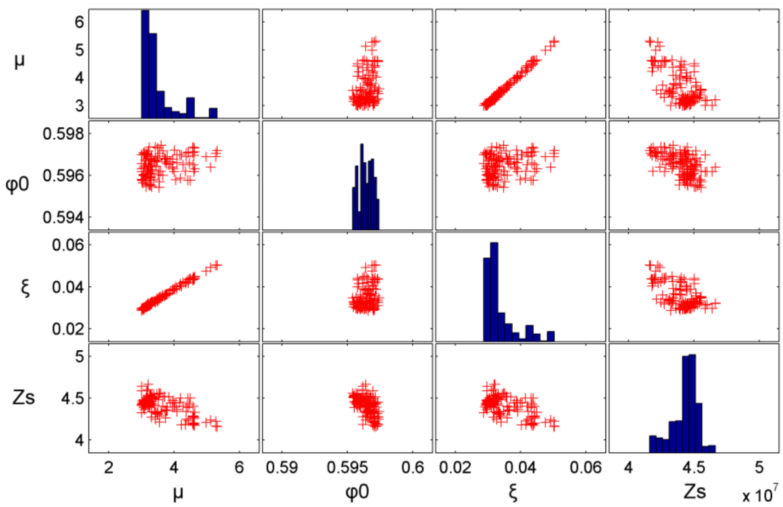

Fig.7 Marginal distributions and two-dimensional correlation plots of posterior parameter samples

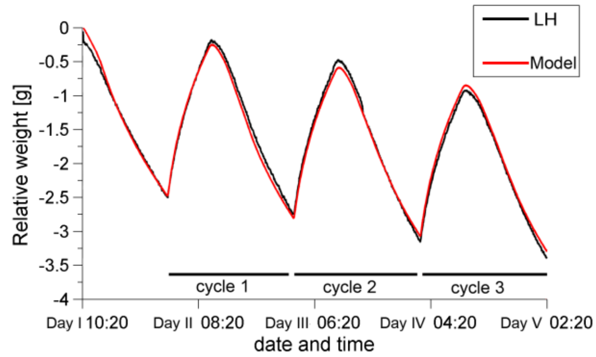

Fig.8 HAM model output with optimized parameters; Relative weight

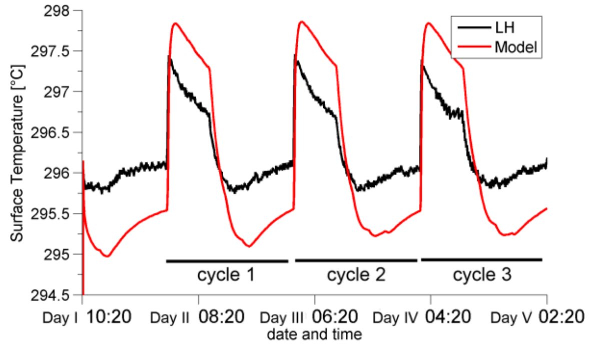

Fig.9 HAM model output with optimized parameters; Surface temperature

7. CONCLUSIONS

(1) The hydraulic binder dosage (Portland cement) seems to have only little influence on hygric properties of LHC in the range 33-75%RH. In fact, the ratio binder/hemp seems to have a larger impact, as the sample with little more hemp in mass proportion (QSH) seems to have a relatively better $MBV_{practical}$. Below 90%RH the surface adsorption of water plays the main role in water storage and the dosage in cement seems to affect only slightly the adsorption potential of LHC. Only the use of a highly hygroscopic binder with high specific area, as clay, could enhance significantly the MBV of such mixes. Concerning water transport, the vapor permeability is influenced mainly by macro-porosity that is also little influenced by the binder itself.
Regarding the thermal properties of the tested bloc, the MBV protocol is unable to give information neither about thermal conductivity nor about thermal capacity. Nevertheless, the proposed protocol shows accurately latent heat effects produced by moisture transfers. Again, the difference between the different binders is not significant here, as they behave all three in a similar way in terms of moisture transfers. It's necessary to find a way of evaluating the impact of such latent effect on the thermal efficiency of such hygroscopic materials
The next step in the research on binder influence on hygric properties would be to explore other relative humidity range to activate other mechanisms (capillary condensation, liquid transport etc.) that could differentiate the different mixes.

(2) The DREAM algorithm showed its efficiency in predicting parameters values for an inverse HAM approach. The model itself proved to be accurate in the MBV cycles prediction and its flexible nature makes it applicable to a large set of building physics problems. As it was shown, the moisture storage and transport parameters are correlated when considered constant but could be replaced by more complex function of the moisture content. Thermal cycles could be also modeled in order to estimate heat transfer parameters like thermal conductivity or capacity.

ACKNOWLEDGEMENT

The authors would like to express their sincere thanks to Isohemp company for their active participation in the samples production.

REFERENCES

1. Evrard, A. and De Herde, A., "Hygrothermal Performance of Lime-Hemp Wall Assemblies," Journal of Building Physics, Vol.34(1), 2010, pp.5-25.
2. Wilkinson, S., "A study of the moisture buffering potential of hemp in combination with lime and clay-based Binders," AEES MSc Thesis Graduate School for Environment, 2009.
3. Fang, L., Clausen, G., Fanger, P.O., "Impact of temperature and humidity on the perception of indoor air quality," Indoor Air, Vol.8(2), 1998, pp.80–90.
4. Peuhkuri, R. H., Mortensen, L. H., Hansen, K. K., Time, B., Gustavsen, A., Ojanen, T., Harderup, L.-E., "Moisture Buffering of Building Materials," In C. Rode (Ed.): Department of Civil Engineering, Technical University of Denmark, 2005.
5. Pedersen, C. R., "A transient model for analyzing the hygrothermal behavior of building constructions," Proceedings of the 3rd IBPSA, Conference, France, 1991.
6. Künzel, H. M., "Simultaneous heat and moisture transport in building components : one- and two-dimensional calculation using simple parameters," IRB Verlag, 1995.
7. Häupl, P., Grunewald, J., Fechner, H., & Stopp, H., "Coupled heat air and moisture transfer in building structures," International Journal of Heat and Mass Transfer, Vol.40(7), 1997, pp.1633-1642.
8. Dos Santos, G. H. and Mendes, N., "Combined Heat, Air and Moisture (HAM) Transfer Model for Porous Building Materials," Journal of Building Physics, Vol.32(3), 2009, pp.203-220.
9. Hagentoft, C.-E., Kalagasidis, A. S., Adl-Zarrabi,

B., Roels, S., Carmeliet, J., Hens, H., Djebbar, R., "Assessment Method of Numerical Prediction Models for Combined Heat, Air and Moisture Transfer in Building Components: Benchmarks for One-dimensional Cases," Journal of Thermal Envelope and Building Science, Vol.27(4), 2004, pp.327-352.

10. Janssens, A., Woloszyn, M., Rode, C., Kalagasidis, A. S., De Paepe, M., "From EMPD to CFD : overview of different approaches for Heat Air and Moisture modeling in IEA Annex 41," Proceedings of the IEA ECBCS Annex 41 Closing Seminar, Conference, Denmark, 2008.
11. Scheffler, G. A. and Plagge, R., "A whole range hygric material model: Modelling liquid and vapour transport properties in porous media," International Journal of Heat and Mass Transfer, Vol.53(1–3), 2010, pp.286-296.
12. Dantas, L. B., Orlande, H. R. B. and Cotta, R. M., "An inverse problem of parameter estimation for heat and mass transfer in capillary porous media," Journal of Heat and Mass Transfer, Vol.46, 2002, pp.1587-1859
13. Metropolis, N., Rosenbluth, A., Rosenbluth, M., Teller, A., Teller, E., "Equation of state calculations by fast computing machines," Journal Chem. Phys., Vol. 21, 1953, pp.1087-1092
14. ter Braak, C. J. F., "A Markov Chain Monte Carlo version of the genetic algorithm Differential Evolution: easy Bayesian computing for real parameter spaces," Statistics and Computing, Vol. 16, 2006, pp.239-249.
15. Vrugt, J., ter Braak, C., Clark, M., Hyman, J., Robinson, B., "Treatment of input uncertainty in hydrologic modeling using adaptive Markov Chain Monte Carlo sampling," Water Ressour. Res. Vol. 44, 2008.
16. Vrugt, J., ter Braak, C., Diks, C., Robinson, B., Hyman, J., Higdon, D., "Accelerating Markov chain Monte Carlo simulation by self adaptive differential evolution with randomized subspace sampling," Int. J. Nonlinear Sci. Numer. Simul. Vol. 10, 2009, pp.271–288.